

Observation of *empty liquids* and *equilibrium gels* in a colloidal clay

Barbara Ruzicka^{1,*}, Emanuela Zaccarelli^{2,*}, Laura Zulian³, Roberta Angelini¹, Michael

Sztucki⁴, Abdellatif Moussaïd⁴, Theyencheri Narayanan⁴, Francesco Sciortino²

¹ CNR-IPCF and Dipartimento di Fisica, Università di Roma La Sapienza, Piazzale A. Moro 2, I-00185, Rome, Italy.

² CNR-ISC and Dipartimento di Fisica, Università di Roma La Sapienza, Piazzale A. Moro 2, I-00185, Rome, Italy.

³ CNR-ISMAC via Bassini 15, 20133 Milan, Italy.

⁴ European Synchrotron Radiation Facility, B.P. 220 F-38043 Grenoble, Cedex France.

*e-mail: barbara.ruzicka@roma1.infn.it; emanuela.zaccarelli@phys.uniroma1.it

The relevance of anisotropic interactions in colloidal systems has recently emerged in the context of the rational design of novel soft materials [1]. Patchy colloids of different shapes, patterns and functionalities [2] are considered the novel building blocks of a bottom-up approach toward the realization of self-assembled bulk materials with pre-defined properties [3–7]. The possibility of tuning the interaction anisotropy will make possible to recreate molecular structures at the nano- and micro- scale (a case with tremendous technological applications), as well as to generate novel unconventional phases, both ordered and disordered. Recent theoretical studies [8] suggest that the phase-diagram of patchy colloids can be significantly altered by limiting the particle coordination number (i.e., valence). New concepts such as empty liquids [8] -liquid states with vanishing density- and equilibrium gels [8–10] -arrested networks of bonded particles, which do not require an underlying phase separation to form [11]- have been formulated. Yet no experimental evidence of these predictions has been provided. Here we report the first observation of empty liquids and equilibrium gels in a complex colloidal clay, and support the experimental findings with numerical simulations.

We investigate dilute suspensions of Laponite, an industrial synthetic clay made of nanometer-sized discotic platelets with inhomogeneous charge distribution and directional interactions. Similarly to other colloidal clays [12–14], Laponite has technological applications in cleansers, surface coatings, ceramic glazes, personal care and cosmetic products, including shampoos and sunscreens [15]. The anisotropy of the face-rim charge interactions combined with the discotic shape of Laponite produce a very rich phase diagram including disordered (gels and glasses) and ordered (nematic) phases, on varying colloidal volume fraction, at fixed ionic strength [15–20]. At low concentrations the system ages very slowly up to a final non-ergodic state [18, 19].

In this work we extend the observation time to time-scales significantly longer than those previously studied and discover that, despite samples appear to be arrested on the second timescale [18, 19], a significant evolution

takes place on the year timescale. Samples undergo an extremely slow, but clear phase separation process into clay-rich and clay-poor phases that are the colloidal analog of gas-liquid phase separation. Spectacularly the phase separation terminates at a finite *but very low* clay concentration, above which the samples remain in a homogeneous arrested state. At variance with respect to the structural transition previously observed for isotropic systems upon a variation of density of depletants [21] this thermodynamic phase transition is driven by a change in colloid density (Laponite concentration). The observed features are instead strikingly similar to those predicted in simple models of patchy particles [8], suggesting that Laponite forms an (arrested) empty liquid at very low concentrations. Furthermore, differently from gels generated by depletion interactions [11, 22] or from molecular glass-formers [23], where arrest occurs after the phase separation process has generated high-density fluctuation regions, here phase separation takes place in a sample which is already a gel.

Fig. 1a-c shows photographs of the temporal evolution of a low concentration Laponite sample (weight concentration $C_w=0.4\%$). The initially fluid suspension (waiting time $t_w=0$) (Fig. 1a) progressively ages, forming a gel (the sample does not flow if turned upside down as evident from Fig. 1b). The gelation time, as probed by dynamic light scattering, depends on clay concentration and it is of the order of few thousand hours for low concentration samples [18]. Waiting significantly longer time (several years), the sample undergoes a phase separation, creating a sharp interface between an upper transparent fluid and a lower opaque gel (Fig. 1c). Phase separation is observed for all samples with $C_w \lesssim 1.0\%$. Fig. 1d shows a photograph of different concentration samples about three years after their preparation. The height of the colloid-rich part (indicated by the dashed lines in Fig. 1d) increases progressively with C_w , filling up the whole sample when $C_w \approx 1.0\%$. This value thus marks the threshold of the phase separation region. We note also that the denser phase in all samples with $C_w < 1.0\%$ approaches $C_w^{gel} \approx 1.0\%$, i.e. exactly the coexisting liquid density, as reported in Fig. 1e. This dense phase retains a memory of the separation process, remaining turbid even at very long times. The turbidity is due to the formation of large density fluctuations, generated during the phase

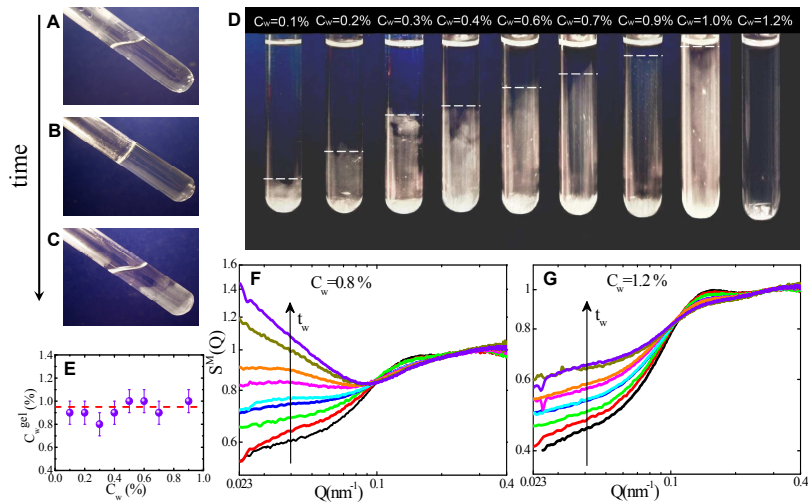


FIG. 1: **Experimental behavior of diluted Laponite suspensions.** **a-c**, Photographs of a $C_w = 0.4\%$ sample **a**, in the initial fluid phase ($t_w = 0$), **b**, in the gel state ($t_w \simeq 4000$ h), **c**, in the phase-separated state ($t_w \approx 30000$ h). **d**, Photographs of samples in the concentration range $0.1 \leq C_w \leq 1.2\%$ at very long waiting times (about 30000 h). All samples with $C_w \leq 1.0\%$ show a clear evidence of two coexisting phases, separated by an interface whose height (dashed horizontal lines) increases progressively with C_w . **e**, Estimated concentration of the denser gel phase in the separated samples shown in panel **d**. **f**, Evolution of the measured $S^M(Q)$ with waiting time for a $C_w = 0.8\%$ sample (located inside the phase separation region). **g**, Evolution of $S^M(Q)$ with waiting time for a $C_w = 1.2\%$ sample (located outside the phase separation region). The curves in panels **f** and **g** are measured at increasing waiting times. From bottom to top: $t_w = 500, 900, 1600, 2700, 3400, 4700, 6000, 8700, 11000$ h.

separation process, whose length scales are comparable to the ones of visible light. Instead, higher concentration samples ($C_w > 1.0\%$) do not show any phase separation and maintain their arrested and transparent character at all times (see $C_w = 1.2\%$ sample in Fig. 1d). Furthermore, no macroscopic changes are observed, in the entire concentration range, in the following four years (seven years, around 60000 hours, in total).

To connect the absence of phase separation and of turbidity in samples above the coexisting liquid density with the proposed equilibrium gel concept [8], as well as to characterize the structural evolution of the phase separation, we have investigated the evolution of the structure of Laponite samples for more than one year. Through Small Angle X-ray Scattering (SAXS) measurements, we have monitored the static structure factor $S^M(Q)$ at different waiting times, from the initial fluid phase up to the gel state (arrested according to light scattering measurements) and during the initial stages of the phase separation process. We have focused on two different concentrations, respectively inside ($C_w = 0.8\%$) and outside ($C_w = 1.2\%$) the phase separation region. The measured $S^M(Q)$ are reported in Fig. 1f and g for different waiting times t_w . At short times $S^M(Q)$ shows a peak, induced by the overall electrostatic repulsion, at $Q \sim 0.15$

nm^{-1} , i.e. a distance of ≈ 40 nm which corresponds to platelets considerably far away one from each other. With increasing t_w , this peak disappears in favor of a new peak emerging at $Q \gtrsim 0.4 \text{ nm}^{-1}$, which corresponds to roughly contacting platelets in a T -configuration ($\lesssim 15$ nm). The shift of the main peak to higher Q values is accompanied by a progressive increase of the intensity at small wave vectors, indicating the onset of aggregation for both concentrations. However with the proceeding of the aging dynamics a drastically different behavior for the two samples is observed: while at $C_w = 0.8\%$ the small Q intensity continuously increases (Fig. 1f), at $C_w = 1.2\%$ the intensity saturates to a constant value at late times (Fig. 1g), as also shown in Fig. S1 in Supplementary Information.

The continuous increase of the small Q behavior of $S^M(Q)$ for $C_w < 1.0\%$ signals the ongoing phase-separation process, revealed also by the sample turbidity. More interesting is the interrupted growth of $S^M(Q)$, accompanied by the formation of a macroscopic gel, which is observed for $C_w > 1.0\%$. Since gelation must occur via a percolation transition, the system has organized itself into a spanning network. The saturation in the evolution of $S^M(Q)$, as time proceeds further, indicates that the system has reached its long-time equilibrium struc-

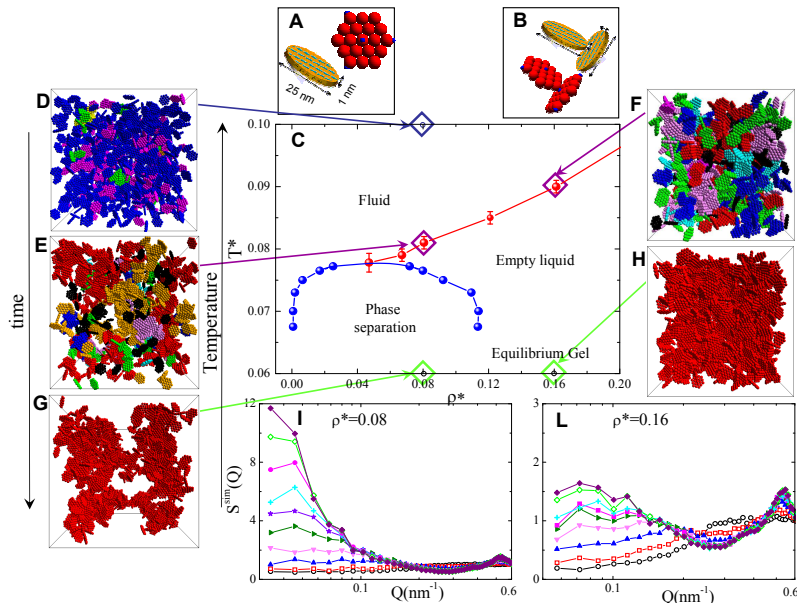


FIG. 2: **Behavior of the patchy particle model for Laponite discs.** **a**, Cartoon of a Laponite platelet and its schematization as a rigid disc composed by 19 sites (red spheres) with 5 attractive patches (blue spheres), three located on the rim and one at the center of each face. **b**, Cartoon representing a T -bonded configuration for two interacting Laponite platelets and its realization in simulations. **c**, Numerical phase diagram: binodal (blue curve) and percolation locus (red curve) in the $\rho^* - T^*$ plane, where ρ^* is the number density scaled by the close-packing density and T^* is the thermal energy scaled by the strength of the bond (see Methods). **d-h**, 3D snapshots of MC simulations at different state points. Different colors correspond to different clusters, and the red-color is reserved for the percolating cluster: **d**, equilibrium fluid phase at $T^* = 0.10$ and $\rho^* \simeq 0.08$; **e,f**, equilibrium configuration at percolation for $\rho^* \simeq 0.08$ and 0.16 ; **g,h**, final gel configurations at $T^* = 0.06$ inside ($\rho^* \simeq 0.08$) and outside ($\rho^* \simeq 0.16$) the phase separation region. In these cases, platelets are connected into a single cluster (gel), which is clearly inhomogeneous (homogeneous) inside (outside) the binodal region. **i,l**, Evolution of the $S^{sim}(Q)$ after a quench at $T^* = 0.06$ for $\rho^* \simeq 0.08$, (inside the phase separation region) and $\rho^* \simeq 0.16$ (outside the phase separation region). Waiting times are: $10^2, 1.2 \times 10^5, 5.7 \times 10^5, 1.6 \times 10^6, 3.6 \times 10^6, 6.1 \times 10^6, 10^7, 2.2 \times 10^7, 4.9 \times 10^7, 1.1 \times 10^8$ in MC steps.

ture, i.e. a stable network. The absence of further structural changes is consistent with the low effective valence of platelets, which at this point have formed most of their possible bonds. Due to the low density of the system, the final gel state is rather non-compact, as signaled by the finite value of $S^M(Q)$ at small Q . During the entire aggregation process the system remains always transparent, confirming that fluctuations on a length scale comparable to the wavelength of light do not develop.

These results suggest that the samples outside the phase separation region reach their equilibrium structure on the year-time scale, while the samples inside the unstable region, despite their apparent gel state, slowly evolve toward complete phase separation. Thus, in Laponite, gelation precedes, but does not preempt, phase separation.

To favor the interpretation of the previous results we introduce a primitive model of patchy discs, which aims to mimic the strong rim-face charge attraction and the tendency of Laponite clay to form open structures. Each platelet is schematized as a hard disk, following the work

of Ref. [24]. To implement the rim-face linking (T -bonds [25, 26]) between different platelets, each disc is decorated with three sites on the rim and one at the center of each face (five sites in total). Only face-rim bonds can form, and they are modeled with a short-range square-well attraction, ensuring that each site can be involved at most in one T -bond. A representation of the model is provided in Fig. 2a and b.

We perform Monte Carlo (MC) and Gibbs ensemble MC (GEMC) simulations to evaluate the gas-liquid coexistence region in the reduced density ρ^* - reduced temperature T^* plane. Fig. 2c shows the binodal line, i.e. the locus of points separating homogeneous and phase-separated state, and the percolation line, defined as the line separating a finite cluster fluid phase (Fig. 2d) from configurations characterized by the presence of a spanning infinite (transient) cluster. Fig. 2e and f show snapshots of the simulated system at the percolation line. Consistently with previously studied patchy-spheres models [8], the gas-liquid coexistence region is confined in a narrow window of T^* and ρ^* . Indeed, the coexisting

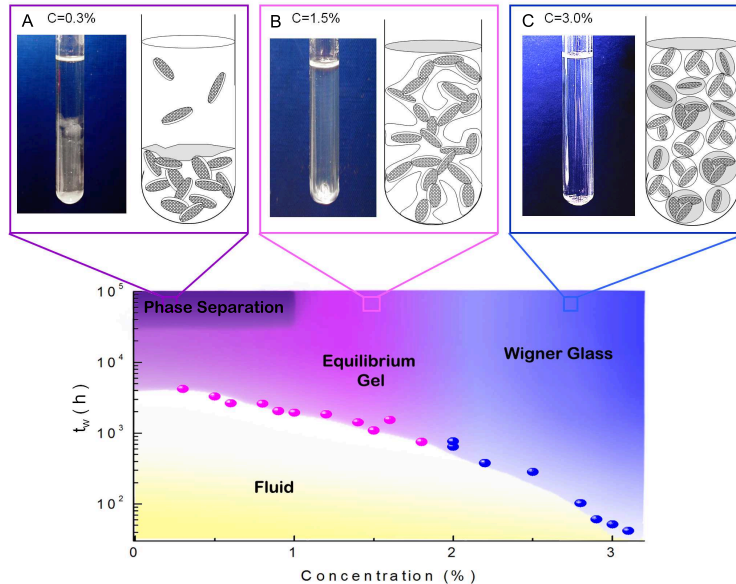


FIG. 3: Phase diagram of diluted Laponite suspensions, in the waiting time vs. concentration plane, resulting from the combined experimental and numerical results. Symbols correspond to experimental t_w values requested to observe non ergodic behavior according to DLS [18]; boundaries inside colored regions are guides to the eye. For long waiting times, three different regions are identified, whose representative macroscopic behavior and a pictorial microscopic view are reported in **a-c**. **a**, Phase-separated sample with colloid-poor (upper part) and colloid-rich (lower part) regions for $C_w \leq 1.0\%$. **b**, Equilibrium gel for $1.0 < C_w < 2.0\%$, characterized by a spanning network of T -bonded discs. **c**, Wigner glass, expected for $2.0 \leq C_w \leq 3.0\%$ [29], where disconnected platelets are stabilized in a glass structure by the electrostatic repulsion, progressively hampering the formation of T -bonds.

liquid density, scaled by the closed packed value, occurs at $\rho^* \approx 0.114$, in significantly dilute conditions. Hence, a wide region of densities exists, above the coexisting liquid density, where the system can be cooled down to very low T without encountering a phase separation, giving rise to an empty liquid state [8]. Such state is composed by an extensively-bonded percolating network that, at low T , restructures itself on a timescale which exceeds the observation time, generating an equilibrium gel state.

We also study the out-of-equilibrium dynamics of the model. To mimic the experimental protocol, we first equilibrate the system at high T (corresponding to sample preparation) and then instantaneously quench it (corresponding to $t_w = 0$) to a sufficiently low T , so that the bond-energy is large as compared to the thermal energy as in Laponite [16]. We propose to interpret the experimental behavior as the low- T limit of our model, connecting the increasing waiting time to a progressive temperature decrease in the numerical study [27]. Snapshots of the final configurations of the system, after a quench inside and outside the phase coexistence region, are shown in Fig. 2g and h. Independently from the density of the quench, the final configuration is always characterized by a single spanning cluster incorporating all particles. The structure of such cluster is highly inhomogeneous for quenches inside the coexistence region

(Fig. 2g) and homogeneous for quenches in the empty liquid region (Fig. 2h). Since at these low T the bond lifetime becomes much longer than the simulation time, the bonded network is persistent, i.e. the system forms a gel.

Fig. 2i,l show the static structure factors calculated from MC configurations $S^{sim}(Q)$ at several times (in MC-steps, equivalent to t_w) following the quench, for two densities, respectively inside and outside the phase separation region. On increasing waiting time the scattered intensity increases in the region of the contact peak (T -bonds, $Q \approx 0.5 \text{ nm}^{-1}$), the peak that monitors the aggregation kinetics, revealing the bond formation process. The notable feature in $S^{sim}(Q)$ is the increase of the scattering at small wavevectors. As in the experimental data, two different scenarios occur at long times after preparation, respectively for samples inside (Fig. 2i) and outside (Fig. 2l) the unstable region. While inside the phase separation region $S^{sim}(Q)$ at small Q increases indefinitely, outside this region the growth stops after a finite waiting time, showing no further evolution.

The zero-th order model introduced here for describing Laponite at low densities condenses the electrostatic interactions between opposite charges into short-ranged attractive sites and neglects the overall repulsive electrostatic interactions, in the spirit of primitive models [28].

These simplifications lead to a different shape of $S(Q)$ at short times – controlled in Laponite by the screened electrostatic interactions [29](see Supplementary Information) — and in the absolute values of $S(Q)$ at small Q . However, the qualitative features shown by the model (Fig. 2i,l) coincide with the ones measured experimentally (Fig. 1f,g) both inside and outside the unstable region, pointing out that our model correctly captures the essential ingredients for describing the experimental behavior. Most importantly, indefinite increase (saturation) in the growth of $S(Q)$ at small Q is seen only inside (outside) the region where phase separation is observed, both in experiments and in simulations.

The present results suggest a novel phase diagram of Laponite suspensions, summarized in Fig. 3, including the crossover taking place for $C_w \sim 2.0\%$ toward a Wigner glass [29]. At low concentrations, for $C_w \lesssim 1.0\%$, the system evolves via a sequence (Fig. 1a-c) of clustering (hours-days), gelation (months) and phase separation (years), from a sol to a homogeneous gel to a phase separated sample in which only the dense phase is arrested. This progression with t_w is strongly reminiscent of a constant-density path in the equilibrium phase diagram in which temperature is progressively decreased and the system evolves from a sol (Fig. 1a, Fig. 2d), to a percolating structure (Fig. 1b, Fig. 2e), finally encountering the phase-separation region (Fig. 1c, Fig. 2g). Differently from the case of isotropic short-range attractive colloids [11] where a homogeneous fluid is driven by a spinodal decomposition into an arrested network, here the system first forms a gel and then the gel extremely slowly increases its local density to fulfill the search for a global free energy minimum (phase separated) state. These features are exactly the ones predicted to take place in patchy colloidal systems when the average valence is small [27], strongly supporting the view that the observed phase-separation is a genuine effect of the directional interactions. The gel phase observed in Laponite above $C_w = 1.0\%$ can thus be interpreted as an arrested empty liquid state, generated by the reduced valence, spontaneously arising from the combination of the platelet shape and the patchy distribution of opposite charges on the disc surface. The observed phase separation on the year time-scale calls attention on the fact that the long term stability of soft materials is controlled by the underlying phase diagram. Knowledge of thermodynamic properties is thus crucial in designing material with desired properties. Our case study shows that a careful choice of the density (within the empty liquid region) may provide materials which are extremely stable in the long term (gels that do not phase separate nor age in the present case), since they are formed continuously from the liquid state, but finally reaching — through a very slow dynamics — their equilibrium configuration.

Methods

Laponite sample preparation Laponite RD suspen-

sions were prepared in a glove box under N_2 flux and were always kept in safe atmosphere to avoid samples degradation [30]. The powder, manufactured by Rockwood Ltd, was firstly dried in an oven at $T=400$ C for 4 hours and it was then dispersed in pure deionized water ($C_s \simeq 10^{-4}$ M), stirred vigorously for 30 minutes and filtered soon after through $0.45 \mu m$ pore size Millipore filters. The same identical protocol has been strictly followed for the preparation of each sample, fundamental condition to obtain reliable and reproducible results [15]. At the end of this preparation process, Laponite forms a colloidal dispersion of charged disk-like particles, with a diameter of ~ 25 nm and a thickness of ~ 1 nm with both negative charges on the faces and positive ones on the rims. The distinct rim and face charges induce a directional face-rim attraction, while a limited valence is realized by means of the additional electrostatic repulsion between like-charges, which inhibits the formation of a large number of bonds per particle. The starting aging time ($t_w=0$) is defined as the time when the suspension is filtered.

The estimate of the denser gel phase concentration C_w^{gel} in the phase-separated samples is provided by the ratio between the nominal concentration and the volume occupied by the dense phase, i.e. neglecting the gas phase concentration.

Small Angle X-ray Scattering Small Angle X-ray Scattering (SAXS) measurements were performed at the High Brilliance beam line (ID2) at the European Synchrotron Radiation Facility (ESRF) in Grenoble, France, using a 10 m pinhole SAXS instrument. The incident x-ray energy was fixed at 12.6 keV. The form factor $F(Q)$ was measured using a flow-through capillary cell. SAXS data were normalized and the scattering background of water was subtracted. The measured structure factor has been obtained as $S^M(Q) = I(Q)/F(Q)$.

Simulations Each platelet is modeled as a hard rigid disk composed of 19 sites on a hexagonal mesh, inspired by the work of [24]. Each site is a hard-sphere of diameter σ , as schematically shown in Fig. 2a. A comparison with Laponite fixes $\sigma = 5$ nm. Each platelet is decorated with five sites, three located symmetrically on the rim and two on the two opposite faces of the central hard-sphere. This primitive model highlights the anisotropic nature of the platelet-platelet interaction [24–26] but neglects the repulsive electrostatic barriers which control the timescale of the aggregation kinetics in Laponite (for a more detailed discussion, see Supplementary Information).

Site-site interactions (acting only between rim and face sites) are modeled as square well interactions, with range 0.1197σ and depth $u_0 = 1$. The number of sites controls the effective valence of the model. Since only rim-face bonds can be formed, the lowest energy state is characterized by an average number of bonds per particle equal to four. The exact choice of the valence controls the loca-

tion of the gas-liquid unstable region, but does not affect the topology of the phase diagram. Indeed, we have verified that upon variation of the number of rim charges, this topology is preserved, in full agreement with the case of spheres decorated by patches [8].

Reduced temperature T^* is the thermal energy scaled by the strength of the bond, $T^* = k_B T / u_0$, where k_B is the Boltzmann constant. Reduced density ρ^* is defined as the number density $\rho = N / L^3$, where N is the number of particle and L the side of the cubic box, scaled by the closed packed density, corresponding to a hexagonal close packing of discs (which is space-filling and equal to $\sqrt{2}/19\sigma^{-3}$). Gibbs Ensemble MonteCarlo (GEMC) simulations are carried out for a system of 250 platelets which partition themselves into two boxes whose total volume is $66603\sigma^3$, corresponding to an average number density $\rho^* \approx 0.05$. At the lowest studied T this corresponds to roughly 235 particles in the liquid box and 15 particles in the gas box (of side 32σ). On average, the code attempts one volume change every five particle-swap moves and 500 displacement moves. Each displacement move is composed of a simultaneous random translation of the particle center (uniformly distributed between $\pm 0.05\sigma$) and a rotation (with an angle uniformly distributed between ± 0.1 radians) around a random axis.

Standard MonteCarlo simulations (MC) are performed for a system of $N = 1000$ platelets in the NVT ensemble. A MC step is defined as N attempted moves (defined as in the GEMC). Each state point is at first equilibrated at $T^* = 0.10$, and then quenched down to $T^* = 0.06$, a temperature well below the critical one, where the system cannot reach equilibrium within the duration of the run. The waiting time is defined as the time of the quench. To reduce numerical noise at each waiting time, the observables of interest, such as the static structure factor $S(Q) = 1/N \langle |\rho_q|^2 \rangle$ with $\rho_q = e^{i\mathbf{Q}\cdot\mathbf{r}}$, are averaged over 10 independent runs.

The use of a square-well potential to model the interactions makes it possible to unambiguously define two platelets as bonded when the pair-wise interaction energy is $-u_0$. Clusters are identified as groups of bonded platelets. To test for percolation, the simulation box is duplicated in all directions, and the ability of the largest cluster to span the replicated system is controlled. If the cluster in the simulation box does not connect with its copy in the duplicated system, then the configuration is assumed to be nonpercolating. The boundary between a percolating and a nonpercolating state point is then defined as the probability of observing infinite clusters in 50% of the configurations.

Acknowledgments BR, LZ, and RA thank G. Ruocco for his constant encouragement and advice during the course of this project. We thank C. De Michele for the code generating the snapshots of Fig. 2 and ESRF for beamtime. EZ and FS acknowledge financial support from ERC-226207-PATCHYCOLLOIDS and ITN-

234810-COMPLOIDS.

Author Contribution BR, LZ, RA performed experiments. MS, AM, TN gave technical support and conceptual advice for the SAXS experiment. EZ and FS did the modeling and numerical simulations. All authors discussed the results and implications and contributed to the writing of the manuscript.

-
- [1] Glotzer, S. C. & Solomon, M. J. Anisotropy of building blocks and their assembly into complex structures. *Nature Mater.* **8**, 557-562 (2007).
 - [2] Pawar, A. B. & Kretzschmar, I. Fabrication, Assembly, and Application of Patchy Particles. *Macromol. Rapid Commun.* **31**, 150-168 (2010).
 - [3] Manoharan, V. N., Elsesser, M. T. & Pine, D. J. Dense packing and symmetry in small clusters of microspheres. *Science* **301**, 483-487 (2003).
 - [4] Zhang, G., Wang, D. & Mohwald, H. Decoration of Microspheres with Gold Nanodots - Giving Colloidal Spheres Valences. *Angew. Chem. Int. Ed.* **44**, 1-5 (2005).
 - [5] Mirkin, C. A., Letsinger, R. L., Mucic, R. C. & Storhoff, J. J. A DNA-based method for rationally assembling nanoparticles into macroscopic materials *Nature* **382**, 607-609 (1996).
 - [6] Kraft, D. J., Groenewold, J. & Kegel, W. K. Colloidal molecules with well-controlled bond angles. *Soft Matter* **5**, 3823-3826 (2009).
 - [7] Nykypanchuk, D., Maye, M. M., van der Lelie, D., & Gang, O. DNA-guided crystallization of colloidal nanoparticles *Nature* **451**, 549-552 (2008).
 - [8] Bianchi, E., Largo, J., Tartaglia, P., Zaccarelli, E. & Sciortino, F. Phase diagram of patchy colloids: towards empty liquids. *Phys. Rev. Lett.* **97**, 168301-168305 (2006).
 - [9] Zaccarelli, E. Colloidal gels: Equilibrium and non-equilibrium routes. *J. Phys. Condens. Matter* **19**, 323101-323151 (2007).
 - [10] Saw, S., Ellegaard, N. L., Kob, W. & Sastry, S. Structural Relaxation of a Gel Modeled by Three Body Interactions. *Phys. Rev. Lett.* **103**, 248305-248309 (2009).
 - [11] Lu, P. J., Zaccarelli, E., Ciulla, F., Schofield, A. B., Sciortino, F. & Weitz, D. A. Gelation of particles with short-range attraction. *Nature* **453**, 499-504 (2008).
 - [12] Brown, A. B. D., Ferrero, C., Narayanan, T. & Rennie, A.R. Phase separation and structure in a concentrated colloidal dispersion of uniform plates. *Eur. Phys. J. B* **11**, 481-489 (1999).
 - [13] Mourad, M. C. D., Byelov, D. V., Petukhov, A. V., de Winter, D. A. M., Verkleij, A. J. & Lekkerkerker H. N. W. Sol-Gel Transitions and Liquid Crystal Phase Transitions in Concentrated Aqueous Suspensions of Colloidal Gibbsite Platelets. *J. Phys. Chem. B* **113**, 11604-11613 (2009).
 - [14] Shalkevich, A., Stradner, A., Bhat, S. K., Muller, F. & Schurtenberger, P. Cluster, Glass, and Gel Formation and Viscoelastic Phase Separation in Aqueous Clay Suspensions. *Langmuir* **23**, 3570-3580 (2007).
 - [15] Cummins H. Z. Liquid, glass, gel: The phases of colloidal Laponite. *J. Non Cryst. Sol.* **353**, 38921-3905 (2007).

- [16] Mourchid, A., Delville, A., Lambard, J., Lecolier, E. & Levitz, P. Phase Diagram of Colloidal Dispersions of Anisotropic Charged Particles: Equilibrium Properties, Structure, and Rheology of Laponite Suspensions. *Langmuir* **11**, 1942-1950 (1995).
- [17] Mongondry, P., Tassin, J. F. & Nicolai, T. Revised state diagram of Laponite dispersions. *J. Colloid Interface Sci.* **283**, 397-405 (2005).
- [18] Ruzicka, B., Zulian, L. & Ruocco, G. Routes to gelation in a clay suspension. *Phys. Rev. Lett.* **93**, 258301 (2004); More on the Phase Diagram of Laponite. *Langmuir* **22**, 1106-1111 (2006).
- [19] Jabbari-Farouji, S., Wegdam, G. H., & Bonn, D. Gels and glasses in a single system: Evidence for an intricate free-energy landscape of glassy materials. *Phys. Rev. Lett.* **99**, 065701-065704 (2007).
- [20] Shahin A. & Joshi, Y. Irreversible Aging Dynamics and Generic Phase Behavior of Aqueous Suspensions of Laponite. *Langmuir* **26**, 4219-4225 (2010).
- [21] Dibble, C. J., Kogan, M. & Solomon, M. J. Structure and dynamics of colloidal depletion gels: Coincidence of transitions and heterogeneity. *Phys. Rev. E* **74**, 041403-041413 (2006); Structural origins of dynamical heterogeneity in colloidal gels. *Phys. Rev. E* **77**, 050401-050404 (2008).
- [22] S. Buzzaccaro, R. Rusconi, R. Piazza, Sticky Hard Spheres: Equation of State, Phase Diagram, and Metastable Gels. *Phys. Rev. Lett.* **99**, 098301-098304 (2007).
- [23] Sastry, S. Liquid Limits: Glass Transition and Liquid-Gas Spinodal Boundaries of Metastable Liquids. *Phys. Rev. Lett.* **85**, 590-593 (1999).
- [24] Kutter, S., Hansen, J.-P., Sprik, M. & Boek, E. Structure and phase behavior of a model clay dispersion: A molecular-dynamics investigation. *J. Chem. Phys.* **112**, 311-322 (2000).
- [25] Dijkstra, M., Hansen, J.-P. & Madden, P. A. Statistical model for the structure and gelation of smectite clay suspensions. *Phys. Rev. E* **55**, 3044-3053 (1997).
- [26] Odriozola, G., Romero-Bastida, M. & Guevara-Rodriguez, F. de J. Brownian dynamics simulations of Laponite colloid suspensions. *Phys. Rev. E* **70**, 021405-021420 (2004).
- [27] Sciortino, F., De Michele, C., Corezzi, S., Russo, J., Zaccarelli, E. & Tartaglia, P. A parameter-free description of the kinetics of formation of loop-less branched structures and gels. *Soft Matter* **5**, 2571-2575 (2009).
- [28] Kolafa, J. & Nezbeda, I. Monte Carlo simulations on primitive models of water and methanol. *Mol. Phys.* **61**, 161-175 (1987).
- [29] Ruzicka, B., Zulian, L., Zaccarelli, E., Angelini, R., Sztucki, M. Moussaïd, A. & Ruocco, G. Competing interactions in arrested states of colloidal clays. *Phys. Rev. Lett* **104**, 085701-085704 (2010).
- [30] Thompson, D. W. & Butterworth, J. T. The Nature of Laponite and its Aqueous Dispersions. *J. Colloid Interface Sci.* **151**, 236-243 (1991).